

# QRPA uncertainties and their correlations in the analysis of $0\nu\beta\beta$ decay

Amand Faessler,<sup>1</sup> G.L. Fogli,<sup>2,3</sup> E. Lisi,<sup>3</sup> V. Rodin,<sup>1</sup> A.M. Rotunno,<sup>2,3</sup> and F. Šimkovic<sup>4,5,1</sup>

<sup>1</sup> *Institute of Theoretical Physics, University of Tuebingen, 72076 Tuebingen, Germany*

<sup>2</sup> *Dipartimento Interateneo di Fisica “Michelangelo Merlin,” Via Amendola 173, 70126 Bari, Italy*

<sup>3</sup> *Istituto Nazionale di Fisica Nucleare, Sezione di Bari, Via Orabona 4, 70126 Bari, Italy*

<sup>4</sup> *Bogoliubov Laboratory of Theoretical Physics, JINR, 141980 Dubna, Russia*

<sup>5</sup> *Department of Nuclear Physics, Comenius University, Mlynská dolina F1, SK-842 15 Bratislava, Slovakia*

The variances and covariances associated to the nuclear matrix elements (NME) of neutrinoless double beta decay ( $0\nu\beta\beta$ ) are estimated within the quasiparticle random phase approximation (QRPA). It is shown that correlated NME uncertainties play an important role in the comparison of  $0\nu\beta\beta$  decay rates for different nuclei, and that they are degenerate with the uncertainty in the reconstructed Majorana neutrino mass.

PACS numbers: 23.40.-s, 23.40.Hc, 21.60.Jz, 02.70.Rr

## I. INTRODUCTION

The search for the neutrinoless mode of double beta decay ( $0\nu\beta\beta$ ),

$$(Z, A) \rightarrow (Z + 2, A) + 2e^-, \quad (1)$$

is being vigorously pursued by several experiments using different  $(Z, A)$  nuclei, in order to unravel the Dirac or Majorana nature of neutrinos and their absolute mass scale [1]. In a given candidate nucleus  $i = (Z, A)$ , light Majorana neutrinos can induce  $0\nu\beta\beta$  decay with half-life  $T_i$  given by

$$T_i^{-1} = G_i |M'_i|^2 m_{\beta\beta}^2 \quad (2)$$

where  $G_i$  is a calculable phase-space factor,  $M'_i$  is the  $0\nu\beta\beta$  nuclear matrix element (NME), and  $m_{\beta\beta}$  is the “effective Majorana neutrino mass,”

$$m_{\beta\beta} = \left| \sum_{k=1}^3 m_k U_{ek}^2 \right|, \quad (3)$$

where  $m_k$  and  $U_{ek}$  are the neutrino masses and the  $\nu_e$  mixing matrix elements, respectively, in standard notation [2]. The NME includes both Fermi (F) and Gamow-Teller (GT) transitions, plus a small tensor (T) contribution [3],

$$M'_i = \left( \frac{g_A}{1.25} \right)^2 \left( M_i^{\text{GT}} + M_i^{\text{T}} - \frac{M_i^{\text{F}}}{g_A^2} \right). \quad (4)$$

In the above expression,  $g_A$  is the effective axial coupling in nuclear matter, not necessarily equal to its “bare” free-nucleon value  $g_A \simeq 1.25$ . With the conventional prefactor  $\propto g_A^2$  in Eq. (4), the phase space  $G_i$  becomes  $g_A$ -independent. In general, all parametric uncertainties (which may be quite large) are embedded in  $|M'_i|$  [4].

It is widely recognized that a convincing case for  $0\nu\beta\beta$  decay must involve independent signals in three or more nuclei [1, 5]. For instance, if the theoretical NME uncertainties could be roughly expressed in terms of a single nuisance parameter  $p$ , then one would need two independent half-life data  $T_1$  and  $T_2$ , and two relations as Eq. (2), to fix both  $p$  and  $m_{\beta\beta}$  (up to degeneracies). A third datum  $T_3$  would overconstrain the system of equations, providing a cross-check of the results [6, 7, 8]. A negative check might signal possible new  $0\nu\beta\beta$  physics beyond light Majorana neutrinos (barring experimental or theoretical mistakes). Any new  $0\nu\beta\beta$  mechanism(s) would then involve at least one more unknown, and thus it might require one or more data  $(T_4, T_5, \dots)$  for further cross-checks [9, 10, 11]. Statistical assessments of the various options demand realistic estimates of experimental and theoretical uncertainties, and the analysis of possible degeneracies which, as we shall see, may play a relevant role.

Recently, there has been significant progress towards the reduction (and a better evaluation) of  $0\nu\beta\beta$  theoretical errors. Within the quasiparticle random phase approximation (QRPA) [3], these uncertainties can be largely kept under control by systematically fixing, in each nucleus, the particle-particle strength parameter  $g_{pp}$  via two-neutrino double beta ( $2\nu\beta\beta$ ) decay rates. In this way, the dispersion of NME values obtained by varying several QRPA ingredients has been significantly reduced (see [4] and references therein).

However, the estimated NME *variances* do not exhaust the information needed to compare  $0\nu\beta\beta$  limits (or signals) in different nuclei: the NME *covariances* are important as well. Nonzero NME covariances have been implicitly recognized in a few works, e.g., by studying the dispersion of NME ratios [8], and by observing that such a dispersion may be smaller than for individual NME [10]. To our knowledge, these observations—implying positive NME correlations—have not yet been sharpened from a statistical viewpoint, despite their relevant consequences for the comparison of  $0\nu\beta\beta$  signals. In a nutshell, the main points can be illustrated as follows. If a finite half-life  $T_i$  is measured in a nucleus  $i$ , the half-life expected in another nucleus  $j$  is

$$T_j = T_i \frac{G_i}{G_j} \frac{|M'_i|^2}{|M'_j|^2}, \quad (5)$$

within (large) NME uncertainties. From the experimental viewpoint, the “most favorable case” would entail the shortest decay timescale  $T_j$ , namely, the smallest  $|M'_i|$  and the largest  $|M'_j|$ . However, if the two NME uncertainties were positively correlated (e.g., via a common normalization factor), opposite changes of  $|M'_i|$  and  $|M'_j|$  would be unlikely, thus preventing the occurrence of the “experimentally favorable” case. Moreover, a common shift of the NME for *all* nuclei could always be compensated by an inverse shift in  $m_{\beta\beta}$  via Eq. (2), leading to a degeneracy between (correlated) theoretical errors and the Majorana neutrino mass.

The purpose of this paper is to explore and discuss these issues in detail. In Sec II we set our notation and conventions. In Sec. III we present our evaluation of the covariance matrix for the NME in a set of nuclei. In Sec. IV we apply our formalism to relevant cases in the  $0\nu\beta\beta$  phenomenology. In Sec. V we summarize our work and discuss future perspectives. An Appendix collects additional details about different theoretical evaluations of  $G_i$  and  $|M'_i|$ .

## II. NOTATION AND CONVENTIONS

In the spirit of Refs. [12, 13, 14], we shall use logarithms of the main  $0\nu\beta\beta$  quantities in appropriate units, namely:

$$\tau_i = \log_{10}(T_i/y), \quad (6)$$

$$-\gamma_i = \log_{10}[G_i/(y^{-1}\text{eV}^{-2})], \quad (7)$$

$$\eta_i = \log_{10}|M'_i|, \quad (8)$$

$$\mu = \log_{10}(m_{\beta\beta}/\text{eV}), \quad (9)$$

so that Eq. (2) is linearized as

$$\tau_i = \gamma_i - 2\eta_i - 2\mu. \quad (10)$$

Central values and errors will be denoted as

$$\tau_i = \tau_i^0 \pm s_i, \quad (11)$$

$$\eta_i = \eta_i^0 \pm \sigma_i, \quad (12)$$

$$\mu = \mu^0 \pm \delta, \quad (13)$$

the  $\gamma_i$  having virtually no uncertainties (see however the Appendix for remarks). Experimental measurements of the  $\tau_i$ 's are thus translated into linear constraints on the unobservable quantity  $\mu$ , once the nuclear matrix elements  $\eta_i$  and their covariances are given.

Linearization through logarithms is appropriate to deal with relatively large NME errors. For instance, a typical “factor of two” uncertainty,  $|M'_i| = |M_i^0| \times (1_{-0.5}^{+1.0})$ , entails at least two drawbacks: (*i*) asymmetric errors are difficult to manage with usual statistical tools (such as least-squares methods); (*ii*) the unphysical region  $|M'_i| < 0$  is hit at twice the lower error. Both drawbacks are avoided by expressing the same “factor of two” uncertainty as  $\eta_i = \eta_i^0 \pm 0.30$ .

Concerning the quantities  $\tau_i = \log_{10}(T_i/y)$ , at present there is only one claim for a positive  $0\nu\beta\beta$  result by Klapdor *et al.* [15, 16] as part of the Heidelberg-Moscow Collaboration:  $T_i/y = 2.23_{-0.31}^{+0.44} \times 10^{25}$  at  $1\sigma$  [16]. We translate this claimed range as

$$\tau_i = 25.355 \pm 0.072 \quad (1\sigma, i = {}^{76}\text{Ge}), \quad (14)$$

where we have slightly displaced the experimental central value so as to reproduce the  $1\sigma$  extrema, by construction, with symmetric errors [17]. For  $n > 1$ , the asymmetric  $n\sigma$  ranges  $T_i/y = 2.23_{-n \cdot 0.31}^{+n \cdot 0.44} \times 10^{25}$  correspond to the symmetric ranges  $\tau_i = 25.355 \pm n \cdot 0.072$  within an acceptable accuracy of 10%, i.e., within about  $0.2\sigma$  ( $0.3\sigma$ ) at the level of  $2\sigma$  ( $3\sigma$ ) ranges.

The above arguments, as well as the advantages of using linear relations [Eq. (10)] and the associated simple statistics (linear propagation of errors,  $\chi^2$  methods), lead us to assume approximately gaussian errors on  $\log z_i$ , rather than on  $z_i$  (where  $z_i = T_i, |M'_i|$ ), for the purposes of this work. In the future, a better knowledge of the probability distributions of the  $z_i$ 's might warrant a different approach, possibly based on more refined statistical tools applicable to generic random variables (maximum likelihood methods, MonteCarlo simulations). However, our main results do not crucially depend on these subtle aspects.

### III. NME UNCERTAINTIES AND THEIR CORRELATIONS

In this Section we discuss estimates for the nuclear matrix elements  $\eta_i$ , in terms of central values  $\eta_i^0$ , errors  $\sigma_i$  and correlations  $\rho_{ij}$ , for a set of eight  $0\nu\beta\beta$  candidate nuclei:  $i = {}^{76}\text{Ge}, {}^{82}\text{Se}, {}^{96}\text{Zr}, {}^{100}\text{Mo}, {}^{116}\text{Cd}, {}^{128}\text{Te}, {}^{130}\text{Te},$  and  ${}^{136}\text{Xe}$ . We remind that the associated covariance matrix is  $\text{cov}(\eta_i, \eta_j) = \rho_{ij}\sigma_i\sigma_j$ , whose diagonal elements coincide with the variances  $\sigma_i^2$ .

#### A. Numerical evaluation

Our estimates are based on a large set of QRPA calculations [4, 18] which include  $2 \times 2 \times 3 \times 2 = 24$  variants in the input ingredients, namely: (i) two values for the axial coupling:  $g_A = 1.25$  (bare) and  $g_A = 1.00$  (quenched); (ii) two approaches to short-range correlations (s.r.c.): the so-called Jastrow-type s.r.c., and the unitary correlation operator method (UCOM); (iii) three sizes for the model basis: small, intermediate and large; (iv) two many-body models: QRPA and its renormalized version (RQRPA). All the 24 variants are supplemented by errors induced by  $g_{pp}$  uncertainties (within the experimental  $2\nu\beta\beta$  constraints). Concerning NME error estimates, we adopt the same conservative approach as in [18], and define the  $1\sigma$  range  $\eta_i^0 \pm \sigma_i$  as the one embracing the minimum and maximum calculated value of  $\eta_i$  for each nucleus  $i$ . These  $\pm 1\sigma$  errors are more generous than their formal statistical definition (which would embrace only  $\sim 68\%$  QRPA variants, i.e.,  $\sim 16$  out of 24). Finally, we calculate the correlation index  $\rho_{ij}$  between joint  $(\eta_i, \eta_j)$  values taken from the same QRPA sample. In all cases, we also include  $g_{pp}$ -induced variations.

Our final results for  $\eta_i$ ,  $\sigma_i$  and  $\rho_{ij}$  are reported in Table I (together with the values of the phase space factors  $\gamma_i$ , for completeness). Figure 1 shows the same results in graphical form, for each couple of different nuclei, in the plane charted by the coordinates  $(\eta_i, \eta_j)$ . In each panel we show the “ $1\sigma$  error ellipse,” centered at  $(\eta_i^0, \eta_j^0)$  and with correlation  $\rho_{ij}$ ; its projection onto a coordinate axis coincide with the  $\pm 1\sigma_i$  range defined previously. Also shown in each panel is the set of QRPA calculations used, supplemented by the horizontal and vertical error bars induced by  $g_{pp}$  uncertainties (for a total of 24 “crosses” in each plane).

In Fig. 1, the strong, positive correlation among theoretical estimates emerges at a glance. The QRPA calculations are mostly scattered along a primary direction (the ellipse major axis) with positive slope, essentially as a result of variations in the s.r.c. model (either Jastrow, blue, or UCOM, red) and, secondarily, to variations in  $g_A$ . There is also some dispersion in the orthogonal direction (ellipse minor axis), which is mainly due to  $g_{pp}$  variations. In general, the overall scatter of QRPA is very well captured by the ellipses, with the possible exception of those involving  $j = {}^{96}\text{Zr}$ , which are somewhat under-sampled at low  $\eta_j$ . For this nucleus, the  $g_{pp}$  parameter turns out to be extremely close to the so-called QRPA collapse point, the  $\eta_j$  estimates becoming less reliable and more erratic as collapse is approached—leading to large and asymmetric error bars. For other nuclei,  $g_{pp}$  is far from the collapse point and the results are more stable (with smaller and more symmetric  $g_{pp}$  errors), as compared to  ${}^{96}\text{Zr}$ . In conclusion, the correlations  $\rho_{ij}$  reported in Table I appear adequate to characterize the scatter of QRPA variants, with the only possible exception of  ${}^{96}\text{Zr}$ , whose estimates must be taken with a grain of salt.

#### B. Comparison with other estimates and discussion

In Fig. 2 (in the same coordinate planes of Fig. 1) we show our error ellipses at 1, 2 and 3 standard deviations ( $\Delta\chi^2 = 1, 4,$  and  $9$ , respectively), and superpose the latest QRPA results from Ref. [19] (dots) and the latest shell-model results from Ref. [20, 21] (stars, for the available nuclei). For each nucleus, these independent  $\eta_i$  evaluations fall within our estimated  $3\sigma$  range,  $\eta_i^0 \pm 3\sigma_i$ ; see also the Appendix for details. Joint estimates of  $(\eta_i, \eta_j)$  for couples of nuclei appear to be roughly aligned along (or parallel to) the major axis of each ellipse, providing an independent confirmation of positive correlations between the NME. The joint estimates also fall within our  $3\sigma$  ellipses in most cases, with a few moderate exceptions in some panels of Fig. 2. We refrain, however, from enlarging our errors (or decreasing their correlations), in order to accommodate these few outliers within each  $3\sigma$  error ellipse. A motivated revision of our estimates should be based on a detailed comparison of our probability distributions with analogous

TABLE I: For each nucleus  $i$ , we report the phase space factor  $\gamma_i$ , the central value of the nuclear matrix error  $\eta_i$ , and the error  $\sigma_i$ , together with the (symmetric) error correlation matrix  $\rho_{ij}$ , according to the QRPA estimates in this work. See the text for definitions.

$i$	$\gamma_i$	$\eta_i^0$	$\sigma_i$	correlation matrix $\rho_{ij}$									
				$^{76}\text{Ge}$	$^{82}\text{Se}$	$^{96}\text{Zr}$	$^{100}\text{Mo}$	$^{116}\text{Cd}$	$^{128}\text{Te}$	$^{130}\text{Te}$	$^{136}\text{Xe}$		
$^{76}\text{Ge}$	25.517	0.635	0.122	1									
$^{82}\text{Se}$	24.870	0.571	0.135	0.978	1								
$^{96}\text{Zr}$	24.550	0.038	0.247	0.518	0.506	1							
$^{100}\text{Mo}$	24.660	0.503	0.162	0.973	0.957	0.491	1						
$^{116}\text{Cd}$	24.622	0.404	0.150	0.961	0.961	0.474	0.965	1					
$^{128}\text{Te}$	26.073	0.534	0.154	0.947	0.968	0.515	0.916	0.930	1				
$^{130}\text{Te}$	26.674	0.498	0.158	0.899	0.927	0.575	0.862	0.870	0.964	1			
$^{136}\text{Xe}$	26.644	0.254	0.187	0.805	0.846	0.663	0.747	0.773	0.898	0.916	1		

ones from independent calculations—rather than with a few sparse points from the published literature. In this sense, it would be useful if other theoretical groups in the  $0\nu\beta\beta$  field could also present “statistical samples” of NME calculations, as suggested in this work.

Some final remarks are in order. As already mentioned, the high correlation in each panel of Fig. 1 is mainly due to the fact that, if the s.r.c. model or the  $g_A$  parameter are varied, all NME tend to either increase or decrease jointly. However, the assumption that  $g_A$  is the same in all nuclei may be too strong, as the amount of quenching might change in different nuclei. In particular, we have shown in [22] that, by using more data besides  $2\nu\beta\beta$  as additional constraints, the fitted values of  $g_A$  is not necessarily constant. Independent variations of  $g_A$  in different nuclei would generally weaken the correlations in Fig. 1. Similarly, nucleus-dependent deformations (ignored in this work) might lead to a further spread of errors and to weaker correlations. In general, for any two given nuclei, the more different their physics (in terms of  $g_{pp}$ ,  $g_A$ , deformation, etc.), the weaker their correlation (in terms of nuclear matrix elements). Our estimated correlations might thus be lowered in the future, should the standard assumptions in QRPA modeling be relaxed in different ways for different nuclei. Despite all these caveats, our  $\rho_{ij}$  matrix represents at least a first, approximate attempt to quantify existing correlations of theoretical uncertainties. Neglecting  $\rho_{ij}$  altogether would definitely lead to worse approximations.

#### IV. APPLICATIONS

In this Section we apply the previous results to cases of practical interest, in order of increasing complexity.

##### A. An application not involving correlations

As a first application (not involving correlations), we translate 90% C.L. limits on half-lives into 90% limits on the Majorana neutrino mass. We remind that a two-sided 90% C.L. range corresponds to  $\pm 1.64\sigma$  ( $\Delta\chi^2 = 2.7$ ); therefore, the claim in Eq. (14) corresponds to

$$\begin{aligned}\tau_i &= \tau_i^0 \pm 1.64 s_i \\ &= 25.355 \pm 0.118 \text{ (90\% C.L., } i = ^{76}\text{Ge)} .\end{aligned}\tag{15}$$

and thus to the following 90% C.L. range for  $\mu$  [as given by Eq. (10)]:

$$\begin{aligned}\mu \pm 1.64\delta &= \frac{1}{2}(\gamma_i - \tau_i^0 \pm 1.64 s_i) - (\eta_i^0 \pm 1.64 \sigma_i) \\ &= -0.554 \pm 0.208 \text{ (90\% C.L., } i = ^{76}\text{Ge)} ,\end{aligned}\tag{16}$$

where the two errors ( $s_i/2$  and  $\sigma_i$ ) have been added in quadrature, being uncorrelated. The corresponding preferred range for the Majorana neutrino mass is:

$$m_{\beta\beta}/\text{eV} = [0.17, 0.45] \text{ (90\% C.L., } i = ^{76}\text{Ge)} .\tag{17}$$

TABLE II: Best current limits on half-lives at 90% C.L. ( $T_i > T_i^{90}$  and  $\tau_i > \tau_i^{90}$ ) for different nuclei  $i$ , from [23].

$i$	$T_i^{90}/y$	$\tau_i^{90}$	Experiment	Ref.
$^{76}\text{Ge}$	$1.6 \times 10^{25}$	25.204	IGEX	[25]
$^{82}\text{Se}$	$2.1 \times 10^{23}$	23.322	NEMO-3	[26]
$^{96}\text{Zr}$	$8.6 \times 10^{21}$	21.934	NEMO-3	[26]
$^{100}\text{Mo}$	$5.8 \times 10^{23}$	23.763	NEMO-3	[26]
$^{116}\text{Cd}$	$1.7 \times 10^{23}$	23.230	Solotvina	[27]
$^{128}\text{Te}$	$7.7 \times 10^{24}$	24.886	Geochem.	[28]
$^{130}\text{Te}$	$3.0 \times 10^{24}$	24.477	CUORICINO	[29]
$^{136}\text{Xe}$	$4.5 \times 10^{23}$	23.653	DAMA	[30]

The best one-sided 90% C.L. limits for various nuclei have been recently reviewed in [23], in terms of half-lives at 90% C.L. ( $\tau_i > \tau_i^{90}$ ), as reported in Table II. It is worth noticing that, if former data from the Heidelberg-Moscow experiment were interpreted as a limit on (rather than a signal of)  $0\nu 2\beta$  decay, the 90% C.L. bound on the  $^{76}\text{Ge}$  half-life would be  $1.9 \times 10^{25}$  y [24], slightly stronger than the one placed by IGEX [25] in Table II.

The information in Table II can be transformed into 90% C.L. limits of the form  $\mu < \mu^{90}$  via the relation

$$\begin{aligned} \mu &< \frac{1}{2}(\gamma_i - \tau_i^{90}) - \eta_i \\ &< \frac{1}{2}(\gamma_i - \tau_i^{90}) - \eta_i^0 + 1.64\sigma_i = \mu^{90} , \end{aligned} \quad (18)$$

where we have linearly added two one-sided limits at 90%: an experimental one ( $-\tau_i^{90}/2$ ) and a theoretical one ( $-\eta_i^{90} + 1.64\sigma_i$ ). In the absence of more detailed information about the (unpublished) probability distribution of experimental  $\tau_i$ 's, this is the most conservative choice.

Figure 3 shows the results of this exercise, in terms of  $m_{\beta\beta}/\text{eV} = 10^\mu$ . The shaded band on the left corresponds to the 90% C.L. range in Eq. (15), while the bands on the right are obtained by inserting the  $\tau_i^{90}$  limits of Table II into Eq. (18), except for the very weak limit from  $^{96}\text{Zr}$  which is out of scale. No experiment appears to have probed the 90% C.L. range preferred by the Klapdor *et al.* claim, although IGEX and CUORICINO have almost reached its lower end.

It is affirmed in [29] that the CUORICINO limit probes part of the Klapdor *et al.* range in  $m_{\beta\beta}$ , seemingly in contrast with our results. However, the arguments in [29] involve a comparison of two *different* confidence levels, namely, the 90% C.L. limit from  $^{130}\text{Te}$  versus the 99.73% C.L. range ( $\pm 3\sigma$ ) from  $^{76}\text{Ge}$ . The latter range is a factor of  $3\sigma/1.64\sigma = 1.83$  wider than the appropriate 90% C.L. range used in Fig. 3 (left side), and thus leads to more optimistic conclusions. In Ref. [14] the comparison was consistently made at the same C.L. for both nuclei, but it involved an intermediate step where correlations were not taken into account (see next subsection), leading again to an optimistic impact for the CUORICINO limit. The analysis proposed in this work shows that, actually, neither IGEX nor CUORICINO exclude fractions of the range claimed in [16] at comparable confidence levels, as far as our estimates for  $\eta_i = \eta_i^0 \pm \sigma_i$  (and  $\rho_{ij}$ ) hold.

## B. Comparison of half-lives in a couple of nuclei

Here we consider a more direct comparison via observable half-lives in two nuclei, bypassing the unobservable Majorana mass  $m_{\beta\beta}$ . We take two different nuclei  $i$  and  $j$ , characterized by nuclear matrix elements  $\eta_i = \eta_i^0 \pm \sigma_i$  and  $\eta_j = \eta_j^0 \pm \sigma_j$  with correlation  $\rho_{ij}$ . A positive  $0\nu\beta\beta$  signal in the first nucleus ( $\tau_i = \tau_i^0 \pm s_i$ ) translates into a favored range for the second nucleus ( $\tau_j = \tau_j^0 \pm s_j$ ) as follows.

From Eq. (10) one obtains, by difference,

$$\tau_j - \tau_i = \Delta_{ij} \pm \epsilon_{ij} , \quad (19)$$

where

$$\Delta_{ij} \equiv \tau_j^0 - \tau_i^0 = (\gamma_j - \gamma_i) + 2(\eta_i^0 - \eta_j^0) , \quad (20)$$

TABLE III: Prospective half-life sensitivities at 90% C.L. ( $T_i^{90}$ ) for different nuclei  $i$  in promising future projects, as reported in [23].

$i$	$T_i^{90}/y$	Project
$^{76}\text{Ge}$	$2.0 \times 10^{26}$	GERDA, MAJORANA
$^{82}\text{Se}$	$2.0 \times 10^{26}$	SuperNEMO
$^{130}\text{Te}$	$2.1 \times 10^{26}$	CUORE
$^{136}\text{Xe}$	$6.4 \times 10^{25}$	EXO

the error  $\epsilon_{ij}$  being obtained by summing in quadrature the correlated uncertainties associated to the difference  $2(\eta_i^0 - \eta_j^0)$ ,

$$\epsilon_{ij}^2 = 4(\sigma_i^2 + \sigma_j^2 - 2\rho_{ij}\sigma_i\sigma_j) . \quad (21)$$

Note that, if the correlation term  $-2\rho_{ij}\sigma_i\sigma_j$  were neglected,  $\epsilon_{ij}$  would be overestimated. The error  $s_j$  associated to  $\tau_j^0 = \tau_i^0 + \Delta_{ij}$  is obtained by summing in quadrature the uncorrelated errors  $s_i$  and  $\epsilon_{ij}$ ,

$$s_i^2 = s_j^2 + \epsilon_{ij}^2 . \quad (22)$$

As a result, the error  $s_j$  has a nonzero correlation  $r_{ij}$  with the error  $s_i$ , as given by  $r_{ij} s_i s_j = s_i^2$ , namely,

$$r_{ij} = \frac{s_i}{s_j} . \quad (23)$$

If we apply the above results to  $i = ^{76}\text{Ge}$  and  $j = ^{130}\text{Te}$ , then the claim by Klapdor *et al.* in Eq. 14,  $\tau_i = 25.355 \pm 0.072$ , implies that  $\tau_j = 24.786 \pm 0.161$ , with error correlation  $r_{ij} = 0.447$ . Figure 4 shows the corresponding error ellipse at  $1.64\sigma$  (90% C.L.), in the plane charted by the  $0\nu\beta\beta$  half-lives of the nuclei  $i = ^{76}\text{Ge}$  and  $j = ^{130}\text{Te}$ . The ellipse can be thought as the combined result of two independent constraints, shown as 90% C.L. bands. The horizontal band corresponds to the experimental claim  $\tau_i = 25.355 \pm (1.64 \times 0.072)$ . The slanted band corresponds to the theoretical limits placed by our QRPA estimates on the ratio  $T_j/T_i$ , namely,  $\tau_j - \tau_i = \Delta \pm (1.64 \times \epsilon_{ij})$ . Note that the projection of the ellipse on the  $x$ -axis provides the range preferred at 90% C.L. for the  $^{130}\text{Te}$  half-life:  $T_j/y = [0.33, 1.12] \times 10^{25}$ . Projections for other nuclei can be similarly derived, as reported in Fig. 5.

Figure 5 shows the two-sided ranges preferred by the Klapdor *et al.* claim at 90% C.L. (shaded rectangles on the right), as well as the one-sided 90% C.L. limits from Table II (bands on the left), for the same nuclei as in Fig. 3. The two-sided limits involve the use of NME errors and correlations, except for  $^{76}\text{Ge}$ , which is a purely experimental input. Once more, we see that none of the existing limits can exclude a fraction of the range favored by Klapdor *et al.* [16] at a comparable confidence level, although IGEX and CUORICINO have almost reached it. The more optimistic claim about the CUORICINO impact in [29] was based on a larger favored range for the  $^{130}\text{Te}$  half-life, as obtained by ignoring correlations in the  $\epsilon_{ij}$  estimate of Eq. (21).

We emphasize that the contents of Figs. 3 and 5, although similar, are not equivalent. The comparison of experimental sensitivities in Fig. 3 is made in terms of a derived quantity ( $m_{\beta\beta}$ ), while in Fig. 5 it is directly made in terms of observables ( $T_i$ ). One-sided bounds in Fig. 3 are obtained by linearly adding 90% C.L. theoretical and experimental limits [Eq. (18)], while in Fig. 5 only the latter limits are used; conversely, theoretical errors are used with full correlation information in the allowed (two-sided) bars of Fig. 5. We think that a comparison in terms of observables, as in Fig. 5, provides a more faithful representation of the current  $0\nu\beta\beta$  decay sensitivities.

We conclude this subsection by discussing the 90% C.L. prospective sensitivities (in terms of  $T_i$ ) of the most promising future  $0\nu\beta\beta$  projects. Table III reports such limits, according to the recent review in Ref. [23]. The values in Table III are largely beyond the two-sided favored ranges in Fig. 5, except perhaps for  $^{136}\text{Xe}$ , where the expected sensitivity is only a factor  $< 2$  beyond the Klapdor *et al.* favored range. This gain may be insufficient if one requires a more demanding check of the claim, at a confidence level significantly higher than 90%. It should be added, however, that all the projects in Table III expect to proceed in a second phase of operation with larger exposures and lower backgrounds, improving the quoted sensitivities by, possibly, another order of magnitude [23].

### C. Combination of half-life data from several nuclei, and degeneracy effects

Let us consider a future, optimistic situation where  $0\nu\beta\beta$  decay is established in  $N$  different nuclei, with measured half-lives

$$\tau_i = \tau_i^0 \pm s_i \quad (i = 1, \dots, N) . \quad (24)$$

Assuming that  $0\nu\beta\beta$  decays proceed only through light Majorana neutrino exchange, these measurements will fix one unknown parameter ( $\mu$ ) via a set of  $N$  linear equations analogous to Eq. (10),

$$\tau_i^0 \pm s_i = \gamma_i - 2(\eta_i^0 \pm \sigma_i) - 2\mu \quad (i = 1, \dots, N) , \quad (25)$$

where the experimental errors  $s_i$  are, in general, uncorrelated (being obtained in independent experiments), while the theoretical errors  $\sigma_i$  have nontrivial correlations  $\rho_{ij}$  (being obtained within the same QRPA model).

This overconstrained system can be solved by the least-squares method, i.e., by minimizing the  $\chi^2$  function

$$\chi^2(\mu) = \sum_{ij} (\tau_i^0 - \gamma_i + 2\eta_i^0 + 2\mu) W_{ij} (\tau_j^0 - \gamma_j + 2\eta_j^0 + 2\mu) , \quad (26)$$

where the weight matrix  $W_{ij}$  is the inverse of the total covariance matrix (including experimental and theoretical errors),

$$[W]_{ij}^{-1} = \delta_{ij} s_i s_j + 4\rho_{ij} \sigma_i \sigma_j . \quad (27)$$

The  $\chi^2$  function is quadratic in  $\mu$ ,

$$\chi^2(\mu) = a\mu^2 + b\mu + c , \quad (28)$$

where

$$a = 4 \sum_{ij} W_{ij} , \quad (29)$$

$$b = 4 \sum_{ij} W_{ij} (\tau_i^0 - \gamma_i + 2\eta_i^0) , \quad (30)$$

$$c = \sum_{ij} (\tau_i^0 - \gamma_i + 2\eta_i^0) W_{ij} (\tau_j^0 - \gamma_j + 2\eta_j^0) . \quad (31)$$

The minimum value  $\chi_{\min}^2$  and the one-sigma shift  $\chi_{\min}^2 + 1$  are reached for  $\mu = \mu_0$  and  $\mu = \mu_0 \pm \delta$ , respectively, where

$$\mu_0 = -\frac{b}{2a} , \quad (32)$$

$$\delta = \frac{1}{\sqrt{a}} , \quad (33)$$

$$\chi_{\min}^2 = c - \frac{b^2}{4a} . \quad (34)$$

The fit is acceptable if  $\chi_{\min}^2/(N-1) \simeq 1$ . Much higher value of  $\chi_{\min}^2$  might signal, e.g., new physics beyond the standard mechanism of  $0\nu\beta\beta$  decay via light Majorana neutrinos (barring experimental and theoretical mistakes). However, the analysis of nonstandard mechanisms is beyond the scope of this work.

As a practical example for the standard  $0\nu\beta\beta$  case, we consider decay searches in each of the four nuclei reported in Table III, in the hypothesis that the true value of  $m_{\beta\beta}$  is 0.2 eV (i.e.,  $\mu = -0.70$ ), close to the lower end of the range in Eq. (17). We assume that the experiments will measure the expected values for the half-lives  $T_i$ ,

$$m_{\beta\beta}/\text{eV} = 0.2 \implies T_i/y = \begin{cases} 4.43 \times 10^{25} & (^{76}\text{Ge}) , \\ 1.34 \times 10^{25} & (^{82}\text{Se}) , \\ 1.20 \times 10^{25} & (^{130}\text{Te}) , \\ 3.43 \times 10^{25} & (^{136}\text{Xe}) , \end{cases} \quad (35)$$

with a fractional uncertainty  $\delta T_i/T_i = 20\%$  (corresponding to  $s_i = 0.08$ ). By construction, the best fit to any combination of these mock data gives back  $\mu_0 = -0.7$  and  $\chi_{\min}^2=0$ . The relevant output parameter is then the reconstructed  $\mu$  uncertainty,  $\delta$ , from Eq. (33).

Table IV shows the  $\delta$  values, for all possible combinations of mock data from the four nuclei (ranging from a single nucleus to all of them). We comment first the results in the 6th column, which are obtained by (incorrectly) switching off correlations, i.e., by setting  $\rho_{ij} = \delta_{ij}$ , as it is often done in the literature.

Without correlations, the error  $\delta$  is given by the familiar combination of total errors from independent data,

$$\frac{1}{\delta^2} = \sum_i \frac{1}{\sigma_i^2 + (s_i/2)^2} \simeq \sum_i \frac{1}{\sigma_i^2}, \quad (36)$$

where we have used the fact that any of the  $\sigma_i$  is a factor of 3–4 greater than  $s_i/2 = 0.04$ . Although the error  $\delta$  is dominated by theoretical uncertainties, it decreases by increasing the data sample (see 6th column of Table IV), as a consequence of (incorrectly) assuming no correlations. Formally, the combination of all the four data would then provide the estimate  $\mu = -0.7 \pm 0.075$ , corresponding to  $m_{\beta\beta} \simeq 0.2 \pm 0.035$ .

Unfortunately, including correlations spoils this nice result. Table IV (last column) shows that, with good approximation, the uncertainty  $\delta$  cannot be much better than the smallest theoretical uncertainty  $\sigma_i$  among the set of nuclei included in the fit. Indeed, even with all four nuclei one obtains  $\delta = 0.127$ , nearly the same as  $\delta = 0.128$  from the single nucleus  $^{76}\text{Ge}$  (characterized by the smallest theoretical error,  $\sigma_i = 0.122$ ). Therefore, regardless of how many accurate experiments are combined, the final accuracy for our test-case Majorana mass will not be better than  $\mu \simeq -0.7 \pm 0.13$ , namely,  $m_{\beta\beta} \simeq 0.2 \pm 0.06$ .

The degeneracy effect induced by correlations can be easily understood in the limiting case of equal and completely correlated theoretical errors ( $\sigma_i \equiv \sigma$  and  $\rho_{ij} \equiv \delta_{ij}$ ). In this case, the QRPA uncertainties would reduce to a common shift  $\eta_i \rightarrow \eta_i + \delta$  for all nuclei, where  $\delta \in [-\sigma, +\sigma]$  within one standard deviation. [In Fig. 1, the ellipses would collapse to “segments” with  $45^\circ$  slope in all panels.] A common shift of all  $\eta_i$  is degenerate with a shift  $\mu \rightarrow \mu - \delta$  via Eq. (10),

$$\tau_i = \gamma_i - 2(\eta_i + \delta) - 2(\mu - \delta), \quad (37)$$

and, thus, the parameter  $\mu$  is affected by an irreducible uncertainty  $\delta = \sigma$ . For unequal NME errors  $\sigma_i$ , the most accurate one dominates in equations like Eq. (37) and thus

$$\delta \simeq \min\{\sigma_i\}, \quad (38)$$

as anticipated.

The difference between  $\delta$  estimates without or with correlations, in the combination of data from  $N$  different nuclei, is striking. Without correlations, and for comparable theoretical uncertainties, the error  $\delta$  would scale as  $\sqrt{N}$  [Eq. (36)]. Including correlations, the error  $\delta$  becomes dominated by the single, most accurate NME, irrespective of  $N$  [Eq. (38)]. One should thus reduce not only the size, but also the correlations of theoretical errors, in order to fully exploit the  $m_{\beta\beta}$  sensitivity of future, multiple-isotope  $0\nu\beta\beta$  searches.

#### D. Prospective constraints on the absolute neutrino mass and Majorana phase

The Majorana mass in  $0\nu\beta\beta$  decay ( $m_{\beta\beta}$ ) is one of the most sensitive probes of the absolute neutrino mass scale  $m_\nu$ , together with the effective neutrino mass in beta decay ( $m_{\beta\beta}$ ) and the sum of the three neutrino masses in cosmology ( $\Sigma$ ); see [14] for updated bounds. It is tempting to combine prospective data on  $(m_{\beta\beta}, m_\beta, \Sigma)$  in the optimistic case of a possible signal “waiting around the corner”, i.e., for masses close to the current *conservative* cosmological bound  $\Sigma \lesssim 0.6$  eV [14, 31, 32]:

$$m_1 \simeq m_2 \simeq m_3 \equiv m_\nu \simeq 0.2 \text{ eV}. \quad (39)$$

For the sake of simplicity, within current neutrino oscillation phenomenology [14], we approximate the mixing matrix values  $U_{ei}^2$  as:

$$U_{e1}^2 \simeq 0.69, \quad (40)$$

$$U_{e2}^2 \simeq 0.31 e^{i\phi}, \quad (41)$$

$$U_{e3}^2 \simeq 0, \quad (42)$$

TABLE IV: Combination of any among the four hypothetical half-life data  $T_i$  in Eq. (35) with experimental uncertainty  $\delta T_i/T_i = 20\%$ . Results are given in terms of the total  $1\sigma$  error  $\delta$  on the parameter  $\mu = \log_{10}(m_{\beta\beta}/\text{eV})$ , including theoretical uncertainties without and with correlations. Bullets indicate the data included in the evaluation (from 1 to 4 data).

# of data	$^{76}\text{Ge}$	$^{82}\text{Se}$	$^{130}\text{Te}$	$^{136}\text{Xe}$	$\delta$ (w/o corr.)	$\delta$ (with corr.)
1	•				0.128	0.128
1		•			0.141	0.141
1			•		0.163	0.163
1				•	0.191	0.191
2	•	•			0.095	0.128
2	•		•		0.100	0.128
2	•			•	0.106	0.127
2		•	•		0.107	0.141
2		•		•	0.114	0.141
2			•	•	0.124	0.163
3	•	•	•		0.082	0.127
3	•	•		•	0.085	0.127
3	•		•	•	0.089	0.127
3		•	•	•	0.093	0.140
4	•	•	•	•	0.075	0.127

where  $\phi$  is an unknown Majorana phase. For nearly degenerate masses it is thus [12]

$$m_\beta \simeq m_\nu, \quad (43)$$

$$\Sigma \simeq 3m_\nu, \quad (44)$$

$$m_{\beta\beta} \simeq m_\nu f, \quad (45)$$

with

$$f \simeq |U_{e1}^2 + U_{e2}^2| \in [0.38, 1], \quad (46)$$

where the upper (lower) end of the range is obtained for the CP-conserving case  $e^{i\phi} = +1$  ( $e^{i\phi} = -1$ ).

Let us test the above scenario with mock data, having the following central values and fractional  $1\sigma$  errors:

$$m_\beta \simeq 0.2(1 \pm 0.5) \text{ eV}, \quad (47)$$

$$\Sigma \simeq 0.6(1 \pm 0.3) \text{ eV}, \quad (48)$$

$$m_{\beta\beta} \simeq 0.2(1 \pm 0.3) \text{ eV}. \quad (49)$$

In the above equations, the 50% uncertainty on  $m_\beta$  corresponds to the smallest  $1\sigma$  error estimated for the upcoming  $\beta$ -decay experiment KATRIN ( $\delta m_\beta \simeq 0.1 \text{ eV}$ ) [33]. A 30% uncertainty on  $\Sigma$  seems appropriate (and even conservative) for a signal in next-generation cosmological data [34, 35]. The putative 30% uncertainty on  $m_{\beta\beta}$  reflects the discussion in the previous subsection.

Combining the “data” in Eqs. (47) and (48), one obtains

$$m_\nu \simeq 0.2(1 \pm 0.25), \quad (50)$$

which, together with Eq. (45) and the “datum” in Eq. (49), imply

$$f \simeq 1 \pm 0.4. \quad (51)$$

This result, compared with the range in Eq. (46), would slightly prefer one CP-conserving case ( $e^{i\phi} = +1$ ) over the other ( $e^{i\phi} = -1$ ), at the level of  $\sim 1.5\sigma$ . Therefore, in an optimistic—but not completely unrealistic—scenario with degenerate neutrino masses, such as the one considered above, a possible determination of  $m_\nu \sim 0.2 \text{ eV}$  with  $\sim 25\%$  accuracy (via  $m_\beta$  plus  $\Sigma$ ) might be accompanied by some indications about the Majorana phase  $\phi$  (via  $m_{\beta\beta}$ ). In this sense, we feel sympathetic towards more encouraging viewpoints [36, 37] than those expressed by a “no-go detection” for  $\phi$  [38], although a real “measurement” of  $\phi$  remains undoubtedly very challenging, even in the most favorable scenarios.

## V. SUMMARY AND PROSPECTS

Nuclear matrix elements for  $0\nu\beta\beta$  decay are affected by relatively large theoretical uncertainties. Within the QRPA approach, we have shown that, within a given set of nuclei, the correlations among NME errors are as important as their size. We have made a first attempt to quantify the covariance matrix of the NME, and to understand its effects in the comparison of current and prospective  $0\nu\beta\beta$  results for two or more nuclei. The effects have been clarified through a series of examples, involving an increasing number of observables. It turns out that correlations may severely limit the accuracy in the reconstruction of  $m_{\beta\beta}$  from any number of  $0\nu\beta\beta$  observations in different nuclei, due to a degeneracy between NME and  $m_{\beta\beta}$  uncertainties. In particular, the fractional error on  $m_{\beta\beta}$  is ultimately dominated by a single fractional NME uncertainty (the smallest one, among the set of nuclei considered). Breaking correlations between different nuclei is thus an important goal, which requires constraining (and improving) the theoretical model of each nucleus by means of many independent data (not only  $2\nu\beta\beta$  data as currently used). In this way, systematic effects common to all nuclei may be reduced. Another relevant goal is to compare correlation estimates in future independent calculations (e.g., QRPA versus shell-model). While pursuing such a long-term theoretical and experimental program, a covariance analysis like the one proposed in this work may represent a useful tool, in order to correctly estimate current or prospective sensitivities to  $0\nu\beta\beta$  decay and to Majorana neutrino parameters.

### Acknowledgments

This work is supported in part by the EU ILIAS project. The work of G.L.F, E.L., and A.M.R. is also supported by the Italian Istituto Nazionale di Fisica Nucleare (INFN) and Ministero dell’Istruzione, dell’Università e della Ricerca (MIUR) through the “Astroparticle Physics” research project. A.F., V.R., and F.Š. acknowledge support of the Transregio SFB Project TR27 “Neutrinos and Beyond” and 436 SLK 17/298 of the Deutsche Forschungsgemeinschaft.

### APPENDIX

This Appendix clarifies the role of different conventions about the  $0\nu\beta\beta$  phase space  $G_i$ , the axial vector coupling  $g_A$ , the nuclear matrix elements  $M'_i$ , and the average nuclear radius parameter  $r_0$ , in comparison with other authors. An agreement on common conventions would be desirable in the future, to avoid possible confusion or ambiguity (see also [39]).

According to usual definitions, the phase space  $G_i$  contains a factor  $(g_A/r_0)^2$ . In this work, the adopted values of  $G_i$  refer to  $r_0 = 1.1$  fm and  $g_A = 1.25$  [40], while changes of  $g_A$  are conventionally embedded in  $M'_i$  (rather than in  $G_i$ ) via the prefactor  $(g_A/1.25)^2$  in Eq. (4) [4, 18]. In order to match such convention, alternative calculations of  $G_i$  using  $r_0 = 1.2$  fm [41, 42, 43] must be rescaled by a factor  $f_0^2 \simeq 1.2$  (where  $f_0 \simeq 1.1 \simeq 1.2/1.1$ ) [39]. Table V compares three different phase-space calculations (in terms of  $G_i m_e^2$ ), all normalized to the same reference values  $g_A = 1.25$  and  $r_0 = 1.1$  fm. One can notice residual differences of  $\sim 5\%$  between the results of [40] and [42, 43], and of  $\sim 10\%$  between those of [40] and [41], presumably due to different approximations used to evaluate the electron wave function and the screening corrections. The (minor) theoretical uncertainties associated to  $G_i$  differences have not been included in this work, but they might become important in the future.

Concerning the nuclear matrix elements  $|M'_i|$ , the values calculated in [19] (QRPA) and [20, 21] (shell model) refer to  $r_0 = 1.2$  fm, and must be rescaled by a factor  $1/f_0$  for comparison with the NME used in this work. Furthermore, since the values in [19] do not embed the prefactor  $(g_A/1.25)^2$ , they must be rescaled by another factor  $1.25^{-2}$  in the subcase  $g_A = 1$ ; this further rescaling is not necessary for the NME values in [21]. Table VI reports the rescaled values of  $|M'_i|$  from [19] and [21] (in terms of logarithms  $\eta_i$ ), as also used in Fig. 2. These  $\eta_i$  values are all contained within our estimated three-standard-deviation ranges  $\eta_i^0 \pm 3\sigma_i$ , which are reported in the last two rows of Table VI.

TABLE V: Comparison of  $G_{im_e}^2$  estimates (in units of  $10^{15} \text{ y}^{-1}$ ) for  $g_A = 1.25$ . The second column refers to the calculations reported in [40] for  $r_0 = 1.1 \text{ fm}$ , as used in this work. The third and fourth columns refer to independent estimates [41, 42, 43] for  $r_0 = 1.2 \text{ fm}$ , rescaled by a compensating factor  $f_0^2 = 1.2$ .

Nucleus	Ref. [40]	Ref. [41]	Refs. [42, 43]
$^{76}\text{Ge}$	7.93	7.67	7.57
$^{82}\text{Se}$	35.2	33.8	32.8
$^{96}\text{Zr}$	73.6	70.2	68.4
$^{100}\text{Mo}$	57.3	54.8	52.8
$^{116}\text{Cd}$	62.3	59.3	56.2
$^{128}\text{Te}$	2.21	2.20	1.99
$^{130}\text{Te}$	55.4	53.2	49.7
$^{136}\text{Xe}$	59.1	56.8	52.4

TABLE VI: Estimates of  $\eta_i = \log_{10} |M'_i|$  for each nucleus, as derived from the recent QRPA calculations in [19] (see Tab. 1 therein) and shell-model calculations in [21] (see Tab. 7 therein) after appropriate rescaling, in order to match the conventions used in this work. The estimates of [21] refer only to a subset of nuclei and to  $g_A = 1.25$ . The s.r.c. used (Jastrow or UCOM) are explicitly reported. The last two rows report the upper and lower ends of our three-standard-deviation ranges  $\eta_i^0 \pm 3\sigma_i$  (for any s.r.c. and  $g_A$ ), which embrace all the above  $\eta_i$  estimates.

Ref.	s.r.c.	$g_A$	$^{76}\text{Ge}$	$^{82}\text{Se}$	$^{96}\text{Zr}$	$^{100}\text{Mo}$	$^{116}\text{Cd}$	$^{128}\text{Te}$	$^{130}\text{Te}$	$^{136}\text{Xe}$
[19]	Jastrow	1.25	0.471	0.313	0.261	0.312	0.331	0.396	0.374	0.222
[19]	UCOM	1.25	0.582	0.427	0.400	0.451	0.435	0.531	0.501	0.335
[19]	Jastrow	1.00	0.564	0.401	0.274	0.396	0.441	0.488	0.435	0.271
[19]	UCOM	1.00	0.687	0.529	0.452	0.553	0.554	0.639	0.584	0.406
[21]	Jastrow	1.25	0.320	0.297				0.328	0.285	0.204
[21]	UCOM	1.25	0.407	0.380				0.418	0.382	0.299
This work	Lower limit at $3\sigma$ level		0.269	0.166	-0.703	0.017	-0.046	0.072	0.024	-0.307
This work	Upper limit at $3\sigma$ level		1.001	0.976	0.779	0.989	0.854	0.996	0.972	0.815

- 
- [1] F. T. Avignone III, S. R. Elliott and J. Engel, “Double Beta Decay, Majorana Neutrinos, and Neutrino Mass,” *Rev. Mod. Phys.* **80**, 481 (2008) [arXiv:0708.1033 [nucl-ex]].
- [2] C. Amsler *et al.* [Particle Data Group], “Review of particle physics,” *Phys. Lett. B* **667**, 1 (2008).
- [3] A. Faessler and F. Šimkovic, “Double beta decay,” *J. Phys. G* **24**, 2139 (1998).
- [4] V. A. Rodin, A. Faessler, F. Simkovic and P. Vogel, “Assessment of uncertainties in QRPA  $0\nu\beta\beta$ -decay nuclear matrix elements,” *Nucl. Phys. A* **766**, 107 (2006) [Erratum-ibid. *A* **793**, 213 (2007)] [arXiv:0706.4304 [nucl-th]].
- [5] K. Zuber, “Summary of the workshop on ‘Matrix elements for neutrinoless double beta decay,’” presented at IPPP Workshop on Matrix Elements for Neutrinoless Double Beta Decay (Durham, England, 2005). arXiv:nucl-ex/0511009.
- [6] S. M. Bilenky and J. A. Grifols, “The possible test of the calculations of nuclear matrix elements of the  $0\nu\beta\beta$  decay,” *Phys. Lett. B* **550**, 154 (2002) [arXiv:hep-ph/0211101].
- [7] S. M. Bilenky, C. Giunti, J. A. Grifols and E. Masso, “Absolute values of neutrino masses: Status and prospects,” *Phys. Rept.* **379**, 69 (2003)
- [8] S. M. Bilenky and S. T. Petcov, “Nuclear matrix elements of  $0\nu\beta\beta$ -decay: Possible test of the calculations,” arXiv:hep-ph/0405237.
- [9] F. Simkovic, “Double beta decay, nuclear structure and physics beyond the standard model,” *Prog. Part. Nucl. Phys.* **57**, 185 (2006).
- [10] F. Deppisch and H. Pas, “Pinning down the mechanism of neutrinoless double beta decay with measurements in different nuclei,” *Phys. Rev. Lett.* **98**, 232501 (2007).
- [11] V. M. Gehman and S. R. Elliott, “Multiple-isotope comparison for determining  $0\nu\beta\beta$  decay mechanisms,” *J. Phys. G* **34**, 667 (2007) [Erratum-ibid. *G* **35**, 029701 (2008)] [arXiv:hep-ph/0701099].
- [12] G. L. Fogli, E. Lisi, A. Marrone, A. Melchiorri, A. Palazzo, P. Serra and J. Silk, “Observables sensitive to absolute neutrino masses: Constraints and correlations from world neutrino data,” *Phys. Rev. D* **70**, 113003 (2004) [arXiv:hep-ph/0408045].
- [13] G. L. Fogli *et al.*, “Observables sensitive to absolute neutrino masses: A reappraisal after WMAP-3y and first MINOS

- results,” Phys. Rev. D **75**, 053001 (2007) [arXiv:hep-ph/0608060].
- [14] G. L. Fogli *et al.*, “Observables sensitive to absolute neutrino masses. II,” Phys. Rev. D **78**, 033010 (2008) [arXiv:0805.2517 [hep-ph]].
- [15] H. V. Klapdor-Kleingrothaus, I. V. Krivosheina, A. Dietz and O. Chkvorets, “Search for neutrinoless double beta decay with enriched Ge-76 in Gran Sasso 1990-2003,” Phys. Lett. B **586**, 198 (2004) [arXiv:hep-ph/0404088].
- [16] H. V. Klapdor-Kleingrothaus and I. V. Krivosheina, “The Evidence For The Observation Of  $0\nu\beta\beta$  Decay: The Identification Of  $0\nu\beta\beta$  Events From The Full Spectra,” Mod. Phys. Lett. A **21**, 1547 (2006).
- [17] G. D’Agostini, “Asymmetric Uncertainties: Sources, Treatment and Potential Dangers,” arXiv:physics/0403086.
- [18] F. Simkovic, A. Faessler, V. Rodin, P. Vogel and J. Engel, “Anatomy of nuclear matrix elements for neutrinoless double-beta decay,” Phys. Rev. C **77**, 045503 (2008) [arXiv:0710.2055 [nucl-th]].
- [19] J. Suhonen and M. Kortelainen, “Nuclear matrix elements for double beta decay,” Int. J. Mod. Phys. E **17**, 1 (2008).
- [20] J. Menendez, A. Poves, E. Caurier and F. Nowacki, “Disassembling the Nuclear Matrix Elements of the Neutrinoless double beta Decay,” arXiv:0801.3760 [nucl-th].
- [21] J. Menendez, A. Poves, E. Caurier and F. Nowacki, “Deformation and the Nuclear Matrix Elements of the Neutrinoless Double Beta Decay,” arXiv:0809.2183 [nucl-th].
- [22] A. Faessler, G. L. Fogli, E. Lisi, V. Rodin, A. M. Rotunno and F. Simkovic, “Overconstrained estimates of neutrinoless double beta decay within the QRPA,” J. Phys. G **35**, 075104 (2008) [arXiv:0711.3996 [nucl-th]].
- [23] A. S. Barabash, “Double beta decay: present status,” Talk at the 13th Lomonosov Conference on Elementary Particle Physics (Moscow, Russia, 2007) arXiv:0807.2948 [hep-ex].
- [24] H. V. Klapdor-Kleingrothaus *et al.*, “Latest results from the Heidelberg-Moscow double-beta-decay experiment,” Eur. Phys. J. A **12**, 147 (2001) [arXiv:hep-ph/0103062].
- [25] C. E. Aalseth *et al.* [IGEX Collaboration], “The IGEX Ge-76 neutrinoless double-beta decay experiment: Prospects for next generation experiments,” Phys. Rev. D **65**, 092007 (2002) [arXiv:hep-ex/0202026].
- [26] A. S. Barabash, “NEMO-3 double beta decay experiment: Latest results,” Proceedings of ICHEP’06, 33rd International Conference on High Energy Physics (Moscow, Russia, 2006), edited by A. Sissakian, G. Kozlov and E. Kolganova (World Scientific, 2007), p. 276. arXiv:hep-ex/0610025; A. S. Barabash [NEMO Collaboration], “NEMO-3 double beta decay experiment: latest results,” talk at NPAE 2008, 2nd International Conference on Current Problems in Nuclear Physics and Atomic Energy (Kyiv, Ukraine, 2008) arXiv:0807.2336 [nucl-ex].
- [27] F. A. Danevich *et al.*, “Search for double beta decay of cadmium and tungsten isotopes: Final results of the Solotvina experiment,” Phys. Rev. C **68**, 035501 (2003).
- [28] T. Bernatowicz, J. Brannon, R. Brazzle, R. Cowsick, C. Hohenberg and F. Podosek, “Precise determination of relative and absolute beta beta decay rates of  $^{128}\text{Te}$  and  $^{130}\text{Te}$ ,” Phys. Rev. C **47**, 806 (1993).
- [29] C. Arnaboldi *et al.* [CUORICINO Collaboration], “Results from a search for the  $0\nu\beta\beta$ -decay of  $^{130}\text{Te}$ ,” Phys. Rev. C **78**, 035502 (2008) [arXiv:0802.3439 [hep-ex]].
- [30] R. Bernabei *et al.*, “Investigation of  $\beta\beta$  decay modes in  $^{134}\text{Xe}$  and  $^{136}\text{Xe}$ ,” Phys. Lett. B **546**, 23 (2002).
- [31] E. Komatsu *et al.* [WMAP Collaboration], “Five-Year Wilkinson Microwave Anisotropy Probe (WMAP) Observations: Cosmological Interpretation,” arXiv:0803.0547 [astro-ph].
- [32] F. De Bernardis, P. Serra, A. Cooray and A. Melchiorri, “An improved limit on the neutrino mass with CMB and redshift-dependent halo bias-mass relations from SDSS, DEEP2, and Lyman-Break Galaxies,” arXiv:0809.1095 [astro-ph].
- [33] E. W. Otten and C. Weinheimer, “Neutrino Mass Limit From Tritium Beta Decay,” Rept. Prog. Phys. **71**, 086201 (2008).
- [34] S. Hannestad and Y. Y. Y. Wong, “Neutrino mass from future high redshift galaxy surveys: Sensitivity and detection threshold,” JCAP **0707**, 004 (2007) [arXiv:astro-ph/0703031].
- [35] J. Lesgourgues and S. Pastor, “Massive neutrinos and cosmology,” Phys. Rept. **429**, 307 (2006) [arXiv:astro-ph/0603494].
- [36] S. Pascoli, S. T. Petcov and T. Schwetz, “The absolute neutrino mass scale, neutrino mass spectrum, Majorana CP-violation and neutrinoless double-beta decay,” Nucl. Phys. B **734**, 24 (2006) [arXiv:hep-ph/0505226].
- [37] F. Deppisch, H. Pas and J. Suhonen, “Double beta decay versus cosmology: Majorana CP phases and nuclear matrix elements,” Phys. Rev. D **72**, 033012 (2005) [arXiv:hep-ph/0409306].
- [38] V. Barger, S. L. Glashow, P. Langacker and D. Marfatia, “No-go for detecting CP violation via neutrinoless double beta decay,” Phys. Lett. B **540**, 247 (2002) [arXiv:hep-ph/0205290].
- [39] S. T. Cowell, “Scaling factor inconsistencies in neutrinoless double beta decay,” Phys. Rev. C **73**, 028501 (2006) [arXiv:nucl-th/0512012].
- [40] F. Simkovic, G. Pantis, J. D. Vergados and A. Faessler, “Additional nucleon current contributions to neutrinoless double beta decay,” Phys. Rev. C **60**, 055502 (1999) [arXiv:hep-ph/9905509].
- [41] J. Suhonen and O. Civitarese, “Weak-interaction and nuclear-structure aspects of nuclear double beta decay,” Phys. Rept. **300**, 123 (1998).
- [42] M. Doi, T. Kotani and E. Takasugi, “Double Beta Decay And Majorana Neutrino,” Prog. Theor. Phys. Suppl. **83**, 1 (1985).
- [43] F. Bohem and P. Vogel, “Physics of Massive Neutrinos” (Cambridge University Press, Cambridge, UK, 1992), 249 pp.

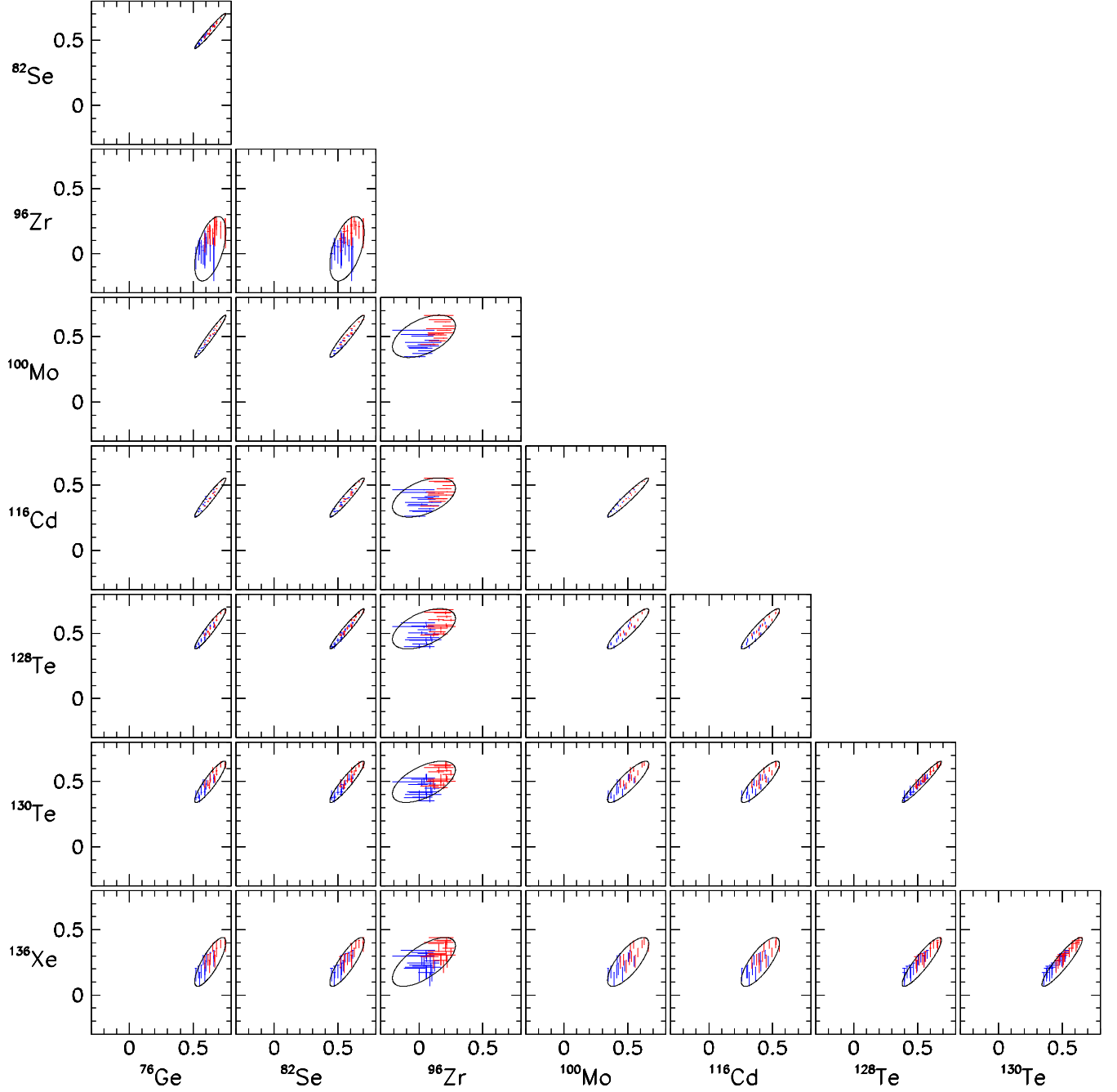


FIG. 1: Scatter plot of estimated QRPA values for the (logarithms of) nuclear matrix elements ( $\eta_i, \eta_j$ ) for each couple of nuclei ( $i, j$ ), together with the error bars induced by  $g_{pp}$  uncertainties. In each panel, also shown is the  $1\sigma$  error ellipse, conservatively estimated on the basis of the scatter plots. See the text for details. Color code for s.r.c: blue (Jastrow), red (UCOM).

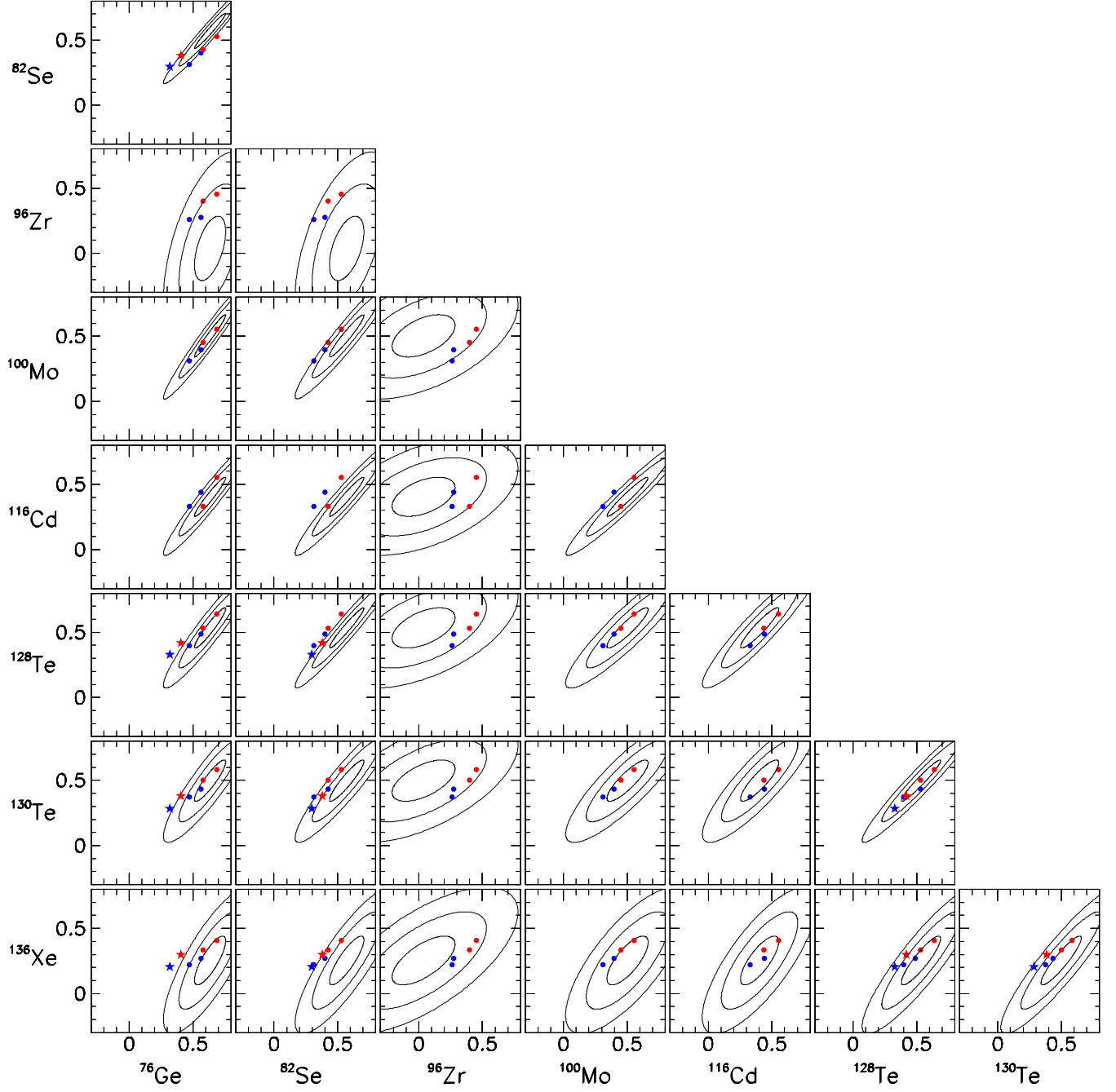


FIG. 2: Error ellipses at  $1\sigma$ ,  $2\sigma$  and  $3\sigma$ , as derived from Fig. 1 and compared with independent nuclear matrix element calculations from [19] (QRPA, dots) and [20] (shell model, stars). Color code for s.r.c: blue (Jastrow), red (UCOM).

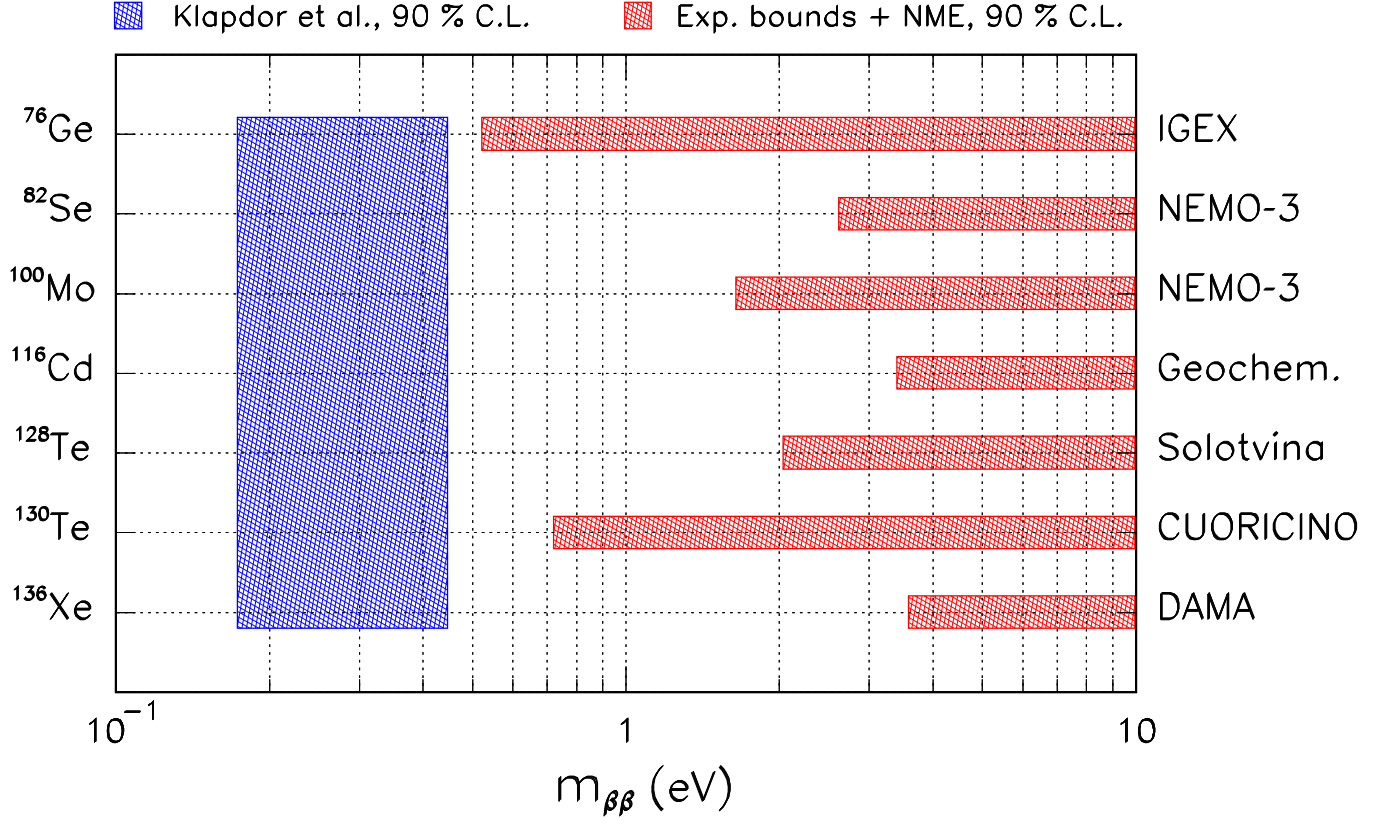


FIG. 3: Range of  $m_{\beta\beta}$  allowed at 90% C.L. by the  $0\nu\beta\beta$  claim of [16], compared with the 90% limits placed by other experiments. The comparison involves the NME and their errors, as estimated in this work.

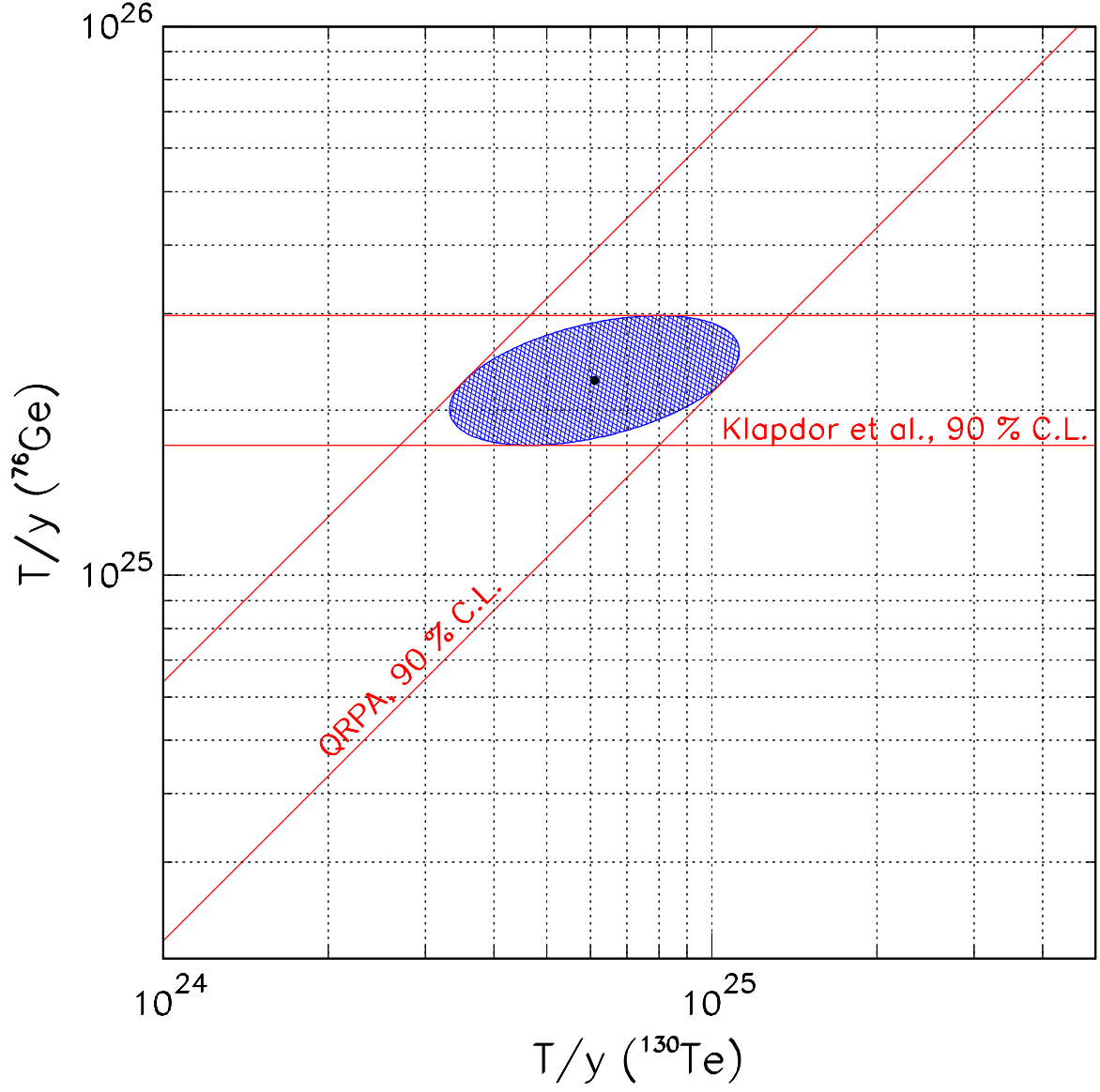


FIG. 4: Example of theoretical and experimental constraints at 90% C.L., in the plane charted by the  $0\nu\beta\beta$  half-lives of  $^{76}\text{Ge}$  and  $^{130}\text{Te}$ . Horizontal band: range preferred by the  $0\nu\beta\beta$  claim of [16]. Slanted band: constraint placed by our QRPA estimates. The combination of the two constraints provides the shaded ellipse, whose projection on the abscissa gives the range preferred at 90% C.L. for the  $^{130}\text{Te}$  half life.

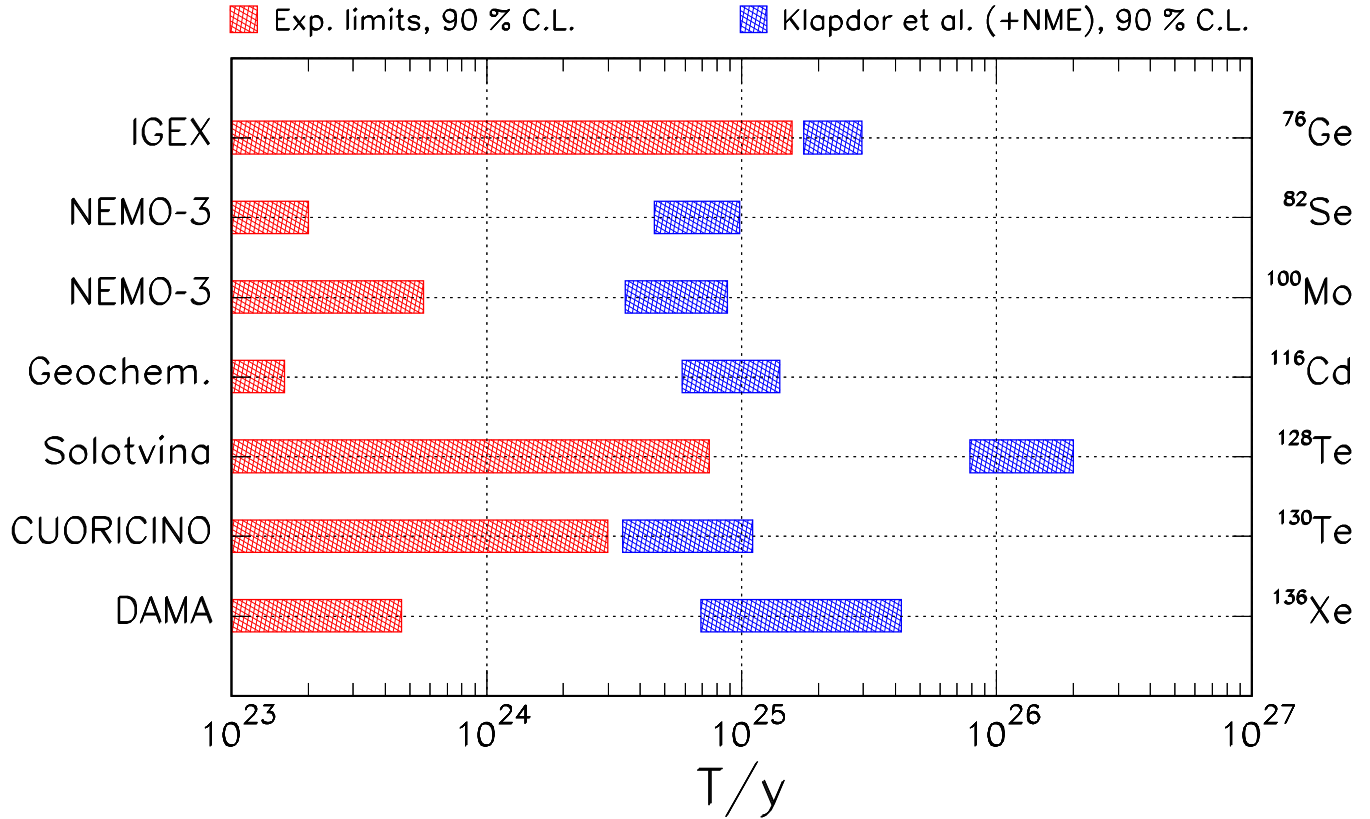


FIG. 5: Range of half-lives  $T_i$  preferred at 90% C.L. by the  $0\nu\beta\beta$  claim of [16], compared with the 90% limits placed by other experiments. The comparison involves the NME and their errors, as well as their correlations, estimated in this work.